Predicting the Failure Response of Cement-Bone Constructs Using a Non-Linear Fracture Mechanics Approach

Kenneth A. Mann[1]
Associate Professor
e-mail: mannk@mail.upstate.edu

Leatha A. Damron
Research Engineer
e-mail: damronl@mail.upstate.edu

Musculoskeletal Sciences Research Center
Department of Orthopedic Surgery
Upstate Medical University
Syracuse, NY 13210

A non-linear fracture mechanics approach was used to predict the failure response of complex cement-bone constructs. A series of eight mechanical tests with a combination of tensile and shear loading along the cement-bone interface was performed. Each experiment was modeled using the finite element method with non-linear constitutive models at the cement-bone interface. Interface constitutive parameters were assigned based on the quantity of bone interdigitated with the cement. There was a strong correlation ($r^2 = 0.80$) between experimentally measured and finite element predicted ultimate loads. The average error in predicted ultimate load was 23.9 percent. In comparison to the ultimate load predictions, correlations and errors for total energy to failure ($r^2 = 0.24$, avg. error $= 38.2$ percent) and displacement at 50 percent of the ultimate load ($r^2 = 0.27$, avg. error $= 52.2$ percent) were poor. The results indicate that the non-linear constitutive laws could be useful in predicting the initiation and progression of interface failure of cemented bone-implant systems. However, improvements in the estimation of post-yield interface properties from the quantity of bone interdigitated with cement are needed to enhance predictions of the overall failure response. [DOI: 10.1115/1.1488167]

Introduction

Debonding of the cement-bone interface in cemented total joint replacements is considered to be an important cause of mechanical failure [1]. In well-fixed femoral components, the cement-bone interface appears to have minimal or no fibrous tissue encapsulation between the cement and bone [2]. Loose components in contrast, often exhibit extensive fibrous encapsulation and loss of interdigitation between cement and bone [3]. The mechanism that causes this change in interface morphology is unclear but is likely to have both mechanical and biologic components [4]. While there have been substantial efforts to understand biologically induced failure mechanisms at the cement-bone interface, particularly those due to osteolysis secondary to implant debris [5,6], there has been limited work to date that elucidates the role of mechanical loading in the failure process.

In a cemented stem application, the cement-bone interface experiences a wide range of tensile, compressive and shear stresses that vary both temporally and spatially. Numerous experiments have been performed to determine the mechanical strength of the interface. These tests have generally been performed to determine the effects of changing surgical technique [7], cement viscosity [8], and cement penetration [9] on mechanical strength. While useful to compare the effects of changing clinically relevant parameters, these strength of materials tests do not provide a direct method to predict the response to mechanical loading.

Fracture mechanics approaches have been used to describe and predict debonding of the cement-bone interface. Linear elastic fracture mechanics (LEFM) methods have been used to characterize the debonding of the cement-bone interface under a variety of loading conditions [10]. In addition, cohesive zones have been added to the LEFM methods to account for the bridging that oc-

curs between the cement and trabecular bone [11]. Both of these approaches assume that the crack tip exhibits small-scale yielding. Short crack lengths and interactions with other boundaries can preclude the validity of LEFM methods [12]. In addition, propagation of cracks along the cement-bone interface in finite element models can require remeshing of the structure during each step of the interface failure process. While this is relatively straightforward for two-dimensional structures, it can become much more challenging for complex three-dimensional models.

Non-linear fracture mechanics methods have recently been used to model the tensile or shear behavior of the cement-bone interface [13,14]. This approach is an extension of the Dugdale-Barenblatt model of crack propagation [15] and has provision for post-yield mechanical softening that is commonly found at this interface. The yielding of the material is assumed to localize along a narrow band of material, while the materials on either side of this band (interface) remained linear elastic. The finite element method was used previously [13,14] to implement this technique with the interface elements exhibiting the appropriate stress versus displacement response.

Structural models of cemented bone-implant systems have used an idealized approach to model failure of the cement-bone interface. Typically, finite element models of cemented stems have assumed a bonded, displacement-compatible cement-bone interface with no provision for failure [16]. When failure was modeled, a fibrous tissue layer was inserted between the cement and bone [17], although the progression of failure was not included. More recently there has been an effort to predict debonding of the cement-bone interface in cemented total hips using multi-axial failure models, but the constitutive models for the interface were not chosen based on detailed mechanics of the cement-bone interface [18]. Thus, at present, we are limited in our abilities to: 1) predict the failure response of the cement-bone interface due to mechanical loading, and 2) assess the effectiveness of predictive finite element models in simulating the failure process.

One difficult problem in predicting the response of the cement-bone interface is the large variations in bone morphology available for interdigitation. Ideally, it would be best to be able to

---

[1]Corresponding author: Dr. K. A. Mann, Department of Orthopedic Surgery, Upstate Medical University, 750 East Adams Street, Syracuse, New York 13210, Ph: (315) 464-9963, Fax: (315) 464-6638.
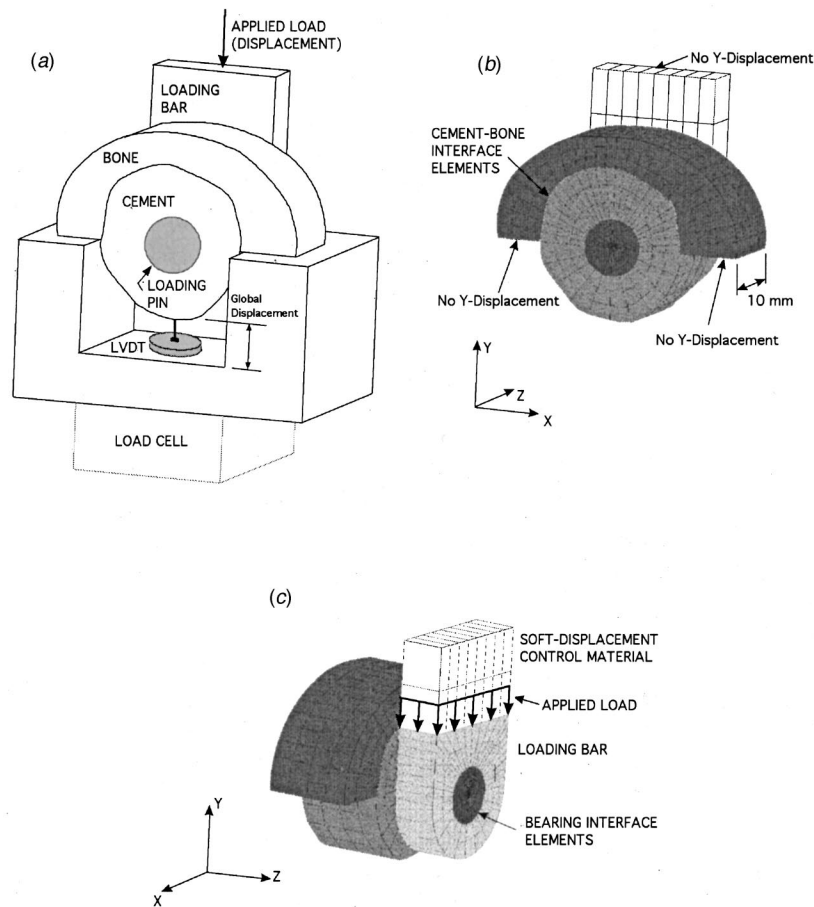
Fig. 1 Experimental (a) and computational models with frontal (b) and oblique side (c) views of the bone-cement section. For a scale reference, the loading pin had a diameter of 6.35 millimeters

predict the mechanical properties of the cement-bone interface in a specific region of the joint replacement using a non-invasive method. A clinically applicable approach analogous to predicting bone mechanical properties using quantitative computed tomography (QCT) would be most useful. To that end, predicting cement-bone interface properties from QCT properties has been performed previously with some success [19]. However, the predictive capabilities of the approach were only moderately successful. The ramifications of this lack of specificity in assigning material properties must be assessed in any predictive model of cement-bone mechanics.

The non-linear fracture mechanics methods, as applied to simple cement-bone specimens, appear promising in reproducing the structural behavior of physical experiments [13]. However, these models have not been applied to more complicated specimens to validate their effectiveness for use in the study of bone-implant systems. Thus, the main goal of this work was to determine if a series of model-specific finite element models (that incorporated the non-linear fracture mechanics approach) could reproduce the failure response of experimentally loaded cement-bone constructs. A secondary aim was to determine how specific changes in the cement-bone interface models, due to lack of specificity of indirect QCT measurements, affected the global structural response of the finite element models. If proven successful, this approach could then be extended to predict the locations of interfacial failure in cemented total joint replacements.

Experimental Methods. A cemented femoral section was chosen as the model geometry for this experiment because it gives a combination of tensile and shear loading along the interface that varies depending on position (Fig. 1A). The cross sectional model also provided direct visualization of the cement-bone failure process. Eight cement-bone constructs were created for mechanical testing from a single fresh-frozen human femur. The femoral head was removed and the canal was broached followed by water lavage. Polymethylmethacrylate cement (Simplex, Stryker-Howmedica-Osteonics, Rutherford, NJ) was mixed under vacuum and introduced into the femoral canal in a retrograde fashion. Proximal pressurization was achieved using a cement impactor. After curing, the femur was sectioned in 10 mm increments, followed by drilling and insertion of a loading pin that was fixed to the cement using epoxy.

The posterior half of the bone section was removed leaving a cement mantle with loading pin and the anterior half of the bone section. The cement was well interdigitated with the trabecular bone in all specimens and the mantle extended to the endosteal cortical wall in each case. A small groove, from front to back, was made at the extent of cement penetration in the lower right corner of the specimen to insure that failure would initiate along one edge of the interface. The specimens were placed in a test fixture on an Instron loading frame (Instron Corporation, Canton, MA) that provided simple supports for the bone. Application of transverse force to the pin was achieved through a rigid loading bar on the back of the specimen using displacement control at a rate of 1 mm/minute. A rotary bearing was used between the loading bar and loading pin to allow the loading pin to rotate freely. The loading bar-loading pin combination produced a uniform displacement of the pin relative to the bone through the thickness of the specimen. The displacement of the base of the cement, below the

loading pin, was monitored throughout the test using an LVDT and applied load was measured using the load cell of the test frame. The resultant load-displacement response was used to indicate the global structural response of each specimen to failure. Three parameters were used to describe each load-displacement curve. The *ultimate load* was the largest load supported by the structure and the *energy to failure* was calculated as the area under the load-displacement curve. To describe the softening response of the structure, the *displacement at 50 percent of the ultimate load* in the softening region was calculated. In addition to the global measure of failure, macrophotographs were taken of each test specimen at several time points throughout the test to further document the experimental failure process. All tests were performed in laboratory air at room temperature. Care was taken to keep the specimen moist during preparation and testing.

Quantifying Cement-Bone Interdigitation. For each specimen we quantified the amount of trabecular bone that was interdigitated with the cement using a multi-step approach [19]. This information was needed to assign material properties to the cement-bone interface in the computational models. A short description of the multi-step approach follows. First, the density of the trabecular bone was estimated using quantitative computed tomography (QCT). Computed tomography scans (General Electric HiSpeed Advantage, Milwaukee, WI) of the femur were made after the femur was broached but before introduction of the cement. Scans were made using a bone algorithm (120 kV, 170 mA, 2s), with 10 mm spacing in the axial direction which corresponded to the physical section locations. The resulting pixel and voxel size was 0.038 mm^2 and 0.190 mm^3, respectively. A dipotassium phosphate phantom $(0–300 \text{ mg/cm}^3 \text{ K}_2\text{HPO}_4)$ was used to convert CT numbers to a representative quantitative computed tomography (QCT) density [20].

After cementing of the femur and sectioning, each section was photographed and scanned as a digital image that could be overlaid with the corresponding CT scan. The photographic images were used to determine the extent of cement penetration (cement line) into the bone. The CT scans were used to define the broach line in the bone because it was often difficult to differentiate the trabecular bone from the cement in this region. These two lines provided the region of bone that was interdigitated with cement. For image analysis, each specimen was evenly divided into six circumferential sectors and the average thickness of interdigitation (t_{int}) was determined for each. The average QCT density of the interdigitated region (ρ_{int}) was also determined for each sector using NIH Image (National Institutes of Health, Bethesda, MD).

Quantity of interdigitated bone (q_{int}) was then determined for each sector using:

$$q_{int} = \rho_{int} * t_{int} \qquad (1)$$

The q_{int} values for each slice surface were used in the finite element models to assign material properties as described below.

Computational Methods: Use of Constitutive Failure Models. The computational models were used to determine if it was possible to reproduce the structural response of the experimental test specimens. To this end, the geometry, material and interface properties were assigned based on parameters that did not require *a priori* physical loading of the experimental specimens. The geometry was obtained from the macrophotographs of the test specimens before mechanical testing and material properties were taken from the literature. Cement-bone interface properties were estimated using data from a previous experiment [21] that was used to determine a relationship between the quantity of interdigitated bone and specific strength and toughness parameters for the interface. Details for each of these steps follow.

Three-dimensional finite element models (Fig. 1B) were created for each of the eight experimental models based on the macrophotographs of the test specimens before mechanical testing. Linear lofting was used between the front and back surfaces of each
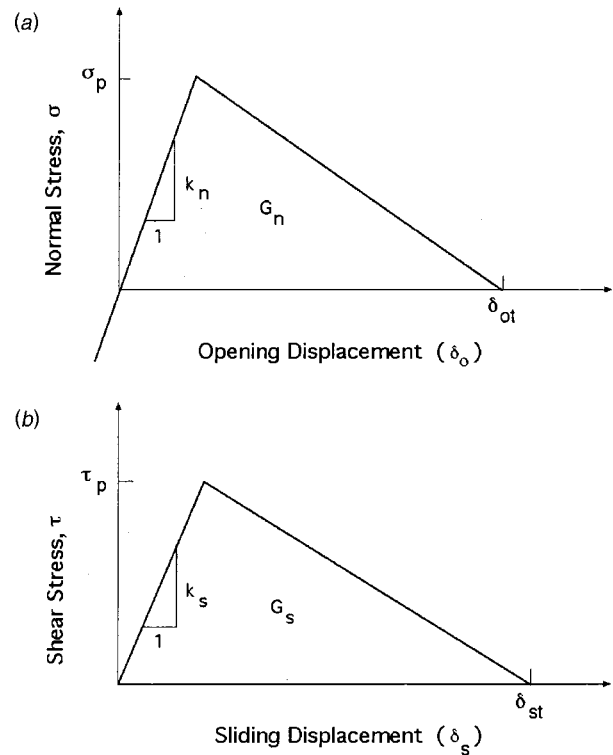
Fig. 2 Interface elements were assigned piece-wise linear constitutive models for both normal direction (a) and shear direction (b) loading

model to create the three-dimensional model. Each model consisted of 1318 fifteen and twenty noded wedge and brick elements with a total of 6503 nodes. The cement, steel loading pin, and steel loading bar were assigned elastic moduli of 2200 MPa [22], 200 GPa, and 200 GPa, respectively. The cortical bone was assigned a modulus of 11500 MPa that is typical for the transverse elastic modulus reported for human cortical bone [23]. The transverse modulus was chosen because this was the primary loading plane for the transverse sections. The cortical bone modulus was not based on the CT scan values because CT measurements typically have not been shown to be good predictors of bone modulus [23]. No regions of trabecular bone were present in the model, except for regions that were interdigitated with the cement. This precluded the need for individual bone properties assigned to trabecular bone. Regions of cement with interdigitated bone were assumed to have the same material properties as the cement. A Poisson's ratio of 0.3 was used for all materials. The model was fixed along the base of the bone to prevent translation in the vertical (y) direction.

Interface elements were placed at the extent of cement penetration into the bone because this was where interfacial failure was found in previous cement-bone mechanical tests [19]. The cement-bone interface elements consisted of three-dimensional, isoparametric, quadratic continuum elements that were modeled as a very thin layer (0.1 mm thick). These elements were initially developed for geotechnical applications [24] and have been applied previously to the study of load transfer in bone implant systems with Coulomb friction interfaces [25,26]. For this study, the cement-bone interface was assigned piece-wise linear constitutive models for loading in out-of-plane normal and in-plane shear directions. The constitutive models were based on a nonlinear fracture mechanics formulation that is an extension of the Dugdale-Barenblatt approach to predicting fracture [27]. In the normal direction, the interface can support tensile loads up to a
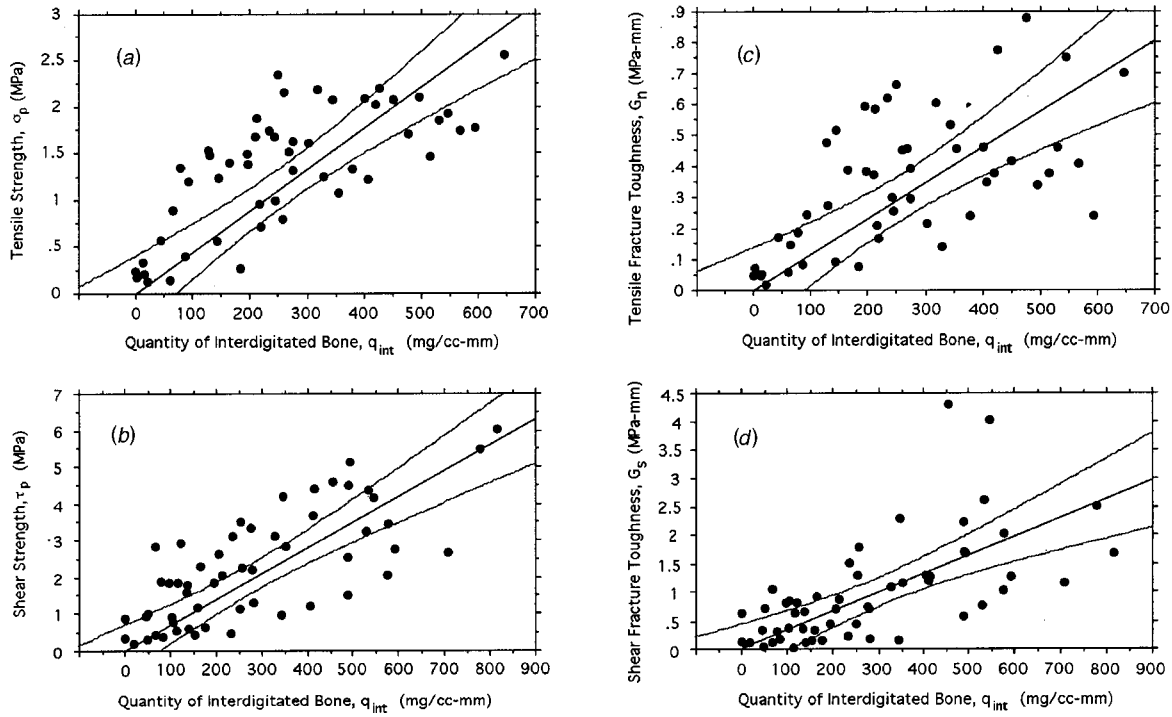
Fig. 3 Tensile strength (a), shear strength (b), tensile fracture toughness (c), and shear fracture toughness (d) results as a function of quantity of interdigitated bone. These relationships were used to assign interface parameters in the present study based on previous data of simple tension and shear specimens [21]. Linear regression results with 99 percent confidence intervals of the mean and slope are shown

peak tensile stress (σ_p) followed by a softening region until the interface no longer supports any load (Fig. 2A). This point is termed the critical interface opening displacement (δ_{ot}). The area under the stress versus opening displacement curve represents the energy absorbed in debonding the interface (G_N) and thus is an indicator of the fracture toughness of the interface. The initial stiffness of the interface in tension (k_n) is chosen to provide the same modulus as the bone cement (22,000 N/mm for the 0.1 mm thick interface). In compression, the interface has the same stiffness as in tension (k_n) and can support infinitely large loads. A similar model is applied in the shear direction (Fig. 2B), except the shear model is anti-symmetric.

The strength and fracture toughness assigned to the interface elements were estimated based on previous experimental data from simple cement-bone test specimens loaded to failure using tension or shear loading [21]. The goal of these previous experiments was to determine a relationship between the quantity of interdigitated bone (q_{int}) at the cement-bone interface and specific test parameters. From these experiments, we found that the strength and fracture toughness could be estimated based on the quantity of interdigitated bone using both tensile and shear loading (Fig. 3). Regression equations:

$$\sigma_p = 0.00443 * q_{int} \quad \text{and} \quad \tau_p = 0.00704 * q_{int} \quad (2)$$

$$G_n = 0.00151 * q_{int} \quad \text{and} \quad G_s = 0.00329 * q_{int} \quad (3)$$

were developed to define the tensile (σ_p) and shear strengths (τ_p), as well as tensile (G_n) and shear (G_s) fracture toughness as linear functions of q_{int}. The correlations between the independent variables and q_{int} were moderate ($r^2 = 0.38$ to 0.5) and were significant ($p < 0.0001$). In the previous work, the softening response of the simple test specimens was not found to correlate well with the quantity of interdigitated bone ($r^2 = 0.012$ to 0.044, $p > 0.5$). Therefore, for the present study a linear softening response was used and the critical opening (δ_{ot}) and sliding (δ_{st}) displacements would be calculated using:

$$\delta_{ot} = 2G_n / \sigma_p \quad \text{and} \quad \delta_{st} = 2G_s / \tau_p \quad (4)$$

It should be noted that the displacement of the interface associated with pre-yield normal (k_n) and shear stiffness (k_s) were negligible when compared to the critical displacements and were not included in Eq. 4. In the finite element models, the cement-bone interface was divided into twelve distinct regions corresponding to the regions measured in the experimental specimens. For the front half of each model, six regions were defined based on q_{int} data from the front face of each physical specimen. For the back half of each model, the six remaining regions were defined based on the q_{int} values for the next adjacent slice.

The load was applied to the loading pin through a loading bar in the same manner as the experiment. To simulate the rotary bearing, interface elements with no-tension and no friction in shear behavior were included at the junction between the loading pin and loading bar (Fig. 1C). A uniform distributed load was applied to the loading bar in the $-y$ direction. An extra layer of low modulus elements was included above the loading bar (Fig. 1C) and was fixed at the top to prevent y translation. The purpose of this layer of elements was to control vertical displacements of the loading bar consistent with the displacement controlled experiment. This additional layer of soft elements therefore served to give the structure an overall positive stiffness, although the cement-bone interface region could actually have a negative tangent stiffness during the softening response. The load through the cement-bone interface was calculated by subtracting the load through the soft layer from the applied load. All analyses were conducted using the finite element code GNOME (Cornell University, Ithaca, NY) using a preconditioned conjugate gradient solver with a global load tolerance of 1.0 percent [24].

Computational Methods: Parametric Study. Two parametric studies were performed to determine the sensitivity of the load-displacement response of the finite element models to changes in interface parameters. The first study evaluated the effect of chang-
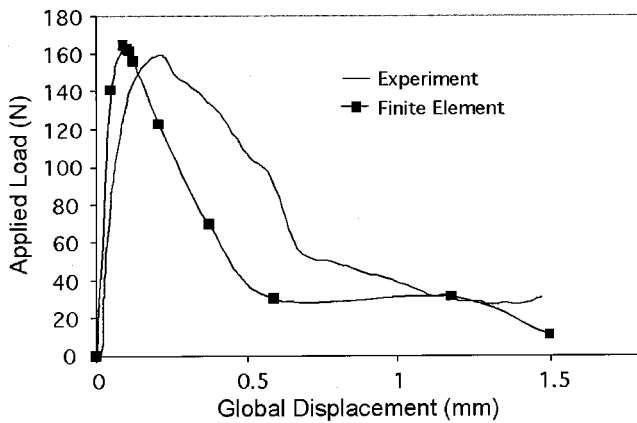
Fig. 4 Typical load versus displacement plot for an experimental test and finite element model

ing the interface strength and fracture toughness independently. For one of the finite element models, the nominal interface strength was increased or decreased by an amount equal to the 99 percent confidence interval values of the q_{int} measures (Fig. 3) while maintaining the fracture toughness at nominal levels. Following this, the fracture toughness was increased or decreased by 99 percent confidence intervals while keeping the interface strength at nominal levels. This approach provided insight into how changes in specific interface parameters affected the overall structural response of the cement-bone specimens. It should be noted that when the interface strength or fracture toughness values were decreased by the 99 percent confidence interval values, some interface strengths were set to zero. This is because at low q_{int}

values, the 99 percent confidence interval bound reaches zero-strength or zero-fracture toughness levels (Fig. 3).

In the second parametric study, we applied the upper 99 percent confidence interval values for strength and fracture toughness to each of the eight finite element models. For each model, the upper confidence interval values of the strength and fracture toughness measures were used in tandem. That is, the upper bound value of interface strength was used along with the upper bound value of fracture toughness. This approach allowed us to account for some of the uncertainty in the q_{int} regression relationships and provided a measure of the bounds of the structural responses that could be expected by these uncertainties.

Experimental Results. The experimental load-displacement responses included linear behavior to a peak load followed by a large post-yield region that supported decreasing loads until the supported load was small (Fig. 4). The experiments were stopped after total displacements of about 1.5 mm and typically a small ligament of the cement-bone interface still supported some load, but this load was small when compared to the peak load carried by the specimen. Seven of the eight specimens exhibited the aforementioned type of response. One specimen had a substantial sudden drop in load coinciding with extensive opening of the cement-bone interface after the ultimate load was reached. Following this episode, structural softening occurred in the same pattern as the remainder of the test specimens. Failure always initiated from the right portion of the interface at the location of the prenotch (Fig. 5). At peak loading, debonding of the cement-bone interface was not noticeable. Progressive failure of the interface corresponded to increasing amounts of structural softening of the load-displacement response.

Ultimate load ($r^2 = 0.70$, $p<0.01$) and energy to failure ($r^2 = 0.76$, $p<0.005$) were significantly and positively correlated with the averaged (average value of 12 regions for each specimen)
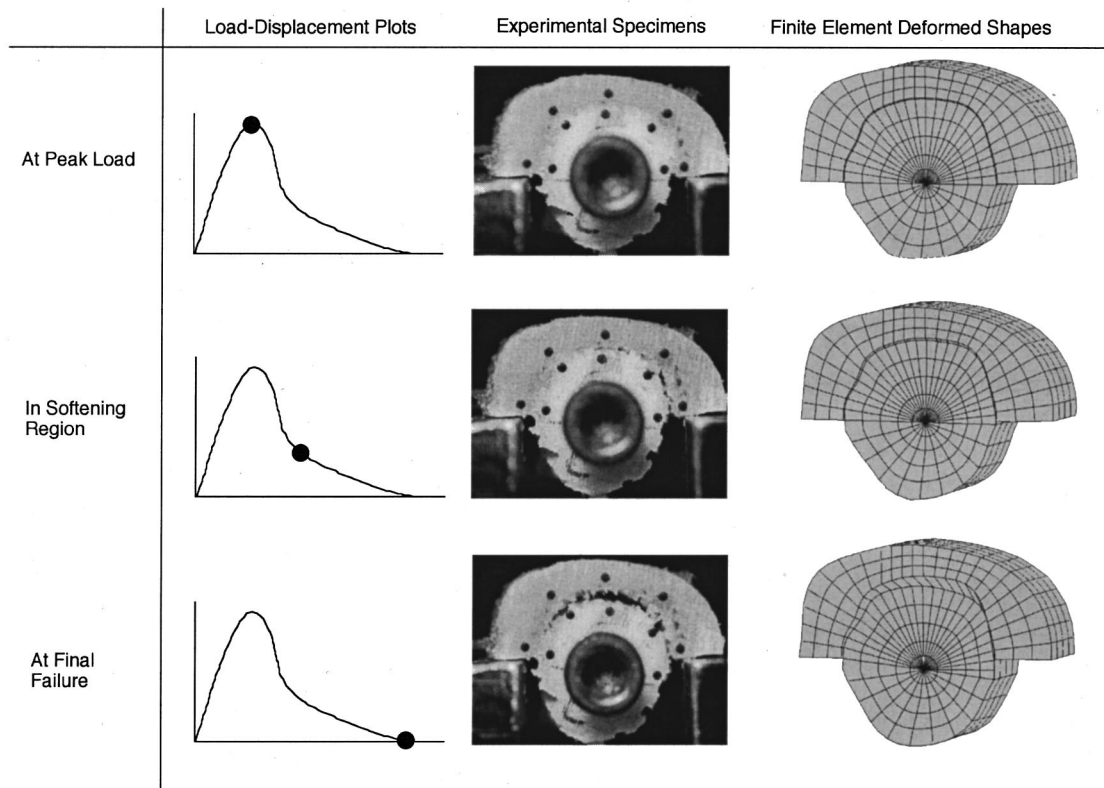
Fig. 5 Displacement behavior of the experiment and corresponding finite element models at peak load (ultimate) in the softening region and at final failure

Table 1 Linear regression relationships and errors between experimentally measured versus finite element predicted structural parameters

Load-Displacement Parameter	Exp. vs. FEA Correlation (r^2)	Exp vs. FEA Significance (Slope)	Mean Error (%)	Error Range (%)
Ultimate Load	0.80	$p<0.003$	23.9	3.1 to 49.9
Energy to Failure	0.23	$p>0.20$	38.2	20.7 to 65.1
Displacement at 50% Ultimate Load	0.27	$p>0.20$	52.2	13.3 to 71.4

quantity of interdigitated bone found at the interface. The relationship between the average quantity of interdigitated bone and the displacement at 50 percent of the ultimate load was not correlated in the experiments ($r^2=0.15$, $p>0.3$).

Computational Results. The finite element models with the non-linear interface constitutive models exhibited a qualitatively similar global load-displacement response when compared to the experiments (Fig. 4). In the example shown, the finite element model resulted in a reasonable estimate of ultimate load, but underestimated the energy to failure and the displacement at 50 percent of the ultimate load. In the models, there was a general linear response to the ultimate load followed by a large region of structural softening until the model supported small or negligible loads. Debonding began on the right side of the cement-bone interface (Fig. 5) and propagated in a similar fashion as the experiment.

Comparison between finite element predictions of structural behavior and actual experimental behavior revealed mixed results. Using linear regression (Table 1), a strong correlation ($r^2=0.80$, $p<0.003$) was found between experiment and finite element predicted ultimate loads (Fig. 6A). Overall the mean error was 23.9 percent. For specimens that failed at lower loads, the errors between predicted and experimental ultimate loads were small. However, at higher failure loads, the finite element models tended to under-predict the ultimate failure load. Using a paired t-test, there was not a significant ($p>0.2$) difference between the ultimate load predicted by the finite element models and that measured in the corresponding experiments.

The finite element results under-predicted the energy to failure for each of the eight test specimens (Fig. 6B) with an average error of 38.2 percent. This difference was statistically significant as tested using a paired t-test ($p<0.01$). The correlation between experimentally measured and predicted energy to failure was poor ($r^2=0.24$) and was not significant ($p>0.2$). The finite element models were least successful in predicting the post-yield (softening) response (Fig. 6C). The errors found comparing the displacement at 50 percent of the ultimate load were the highest of all of the parameters (52.2 percent). The finite element models predicted significantly lower displacement at 50 percent of the ultimate load when compared to the experiments ($p<0.005$). Correlations between model and experiment for this parameter were weak ($r^2=0.27$) and not significant ($p>0.2$). This indicates that the finite element models were quantitatively least effective in capturing the structural behavior of the post-yield response.

Results from the Parametric Studies. Changing the magnitudes of the interface model parameters did not have a straightforward effect on the structural response of the cement-bone specimens. Increasing the interface strength by 99 percent confidence interval values increased the ultimate load by 13.5 percent (Fig. 7A), whereas decreasing the interface strength by the 99 percent confidence interval values resulted in a 37.9 percent decrease in the ultimate load (Table 2). This is thought to be due to the fact that at low q_{int} levels the lower 99 percent confidence interval band actually predicts zero strength. Thus numerous elements at the interface were assigned properties with no strength in this case. Adjusting the interface strength by the 99 percent confidence interval levels did not have as large an effect on the predicted energy to failure, but had a marked effect on the displace-
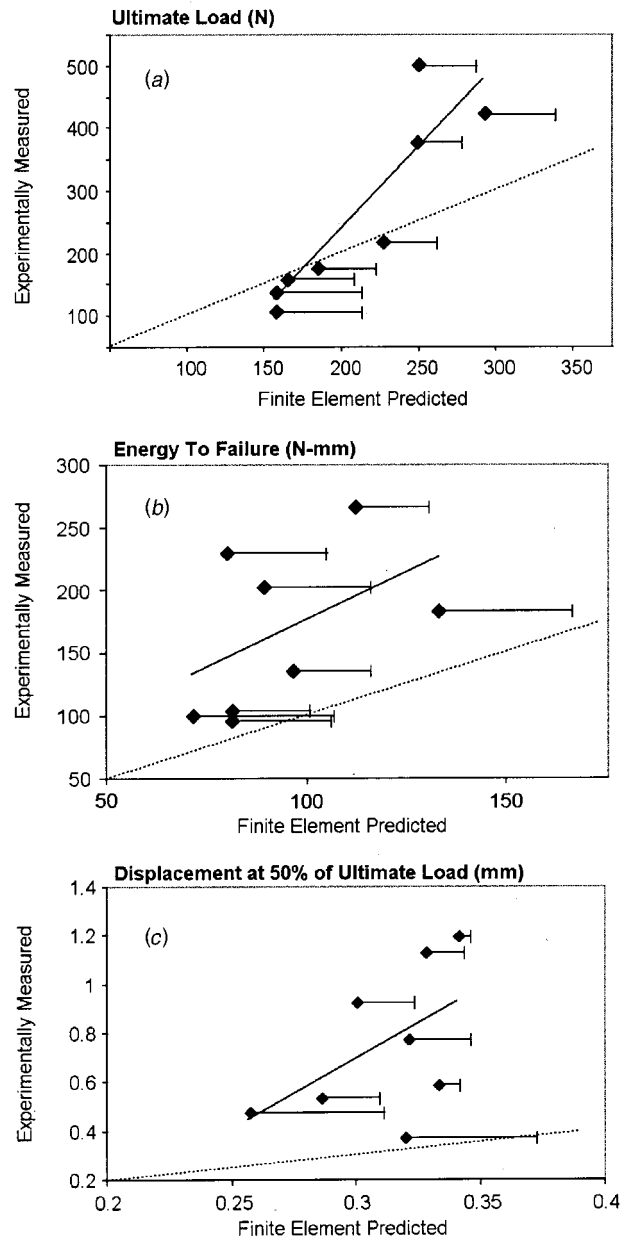
Fig. 6 Comparison between experimental measurements and finite element predictions for the eight test specimens. Results for ultimate load (a), energy to failure (b) and displacement at 50 percent of the ultimate load (c) are shown. Error bars represent results for models using interface parameters determined at +99 percent confidence intervals for interface strength and fracture toughness (see Fig. 4). A regression line for the experiment versus finite element prediction is shown as a solid line. The dotted line indicates a perfect correspondence (unity slope) between experiment and finite element results
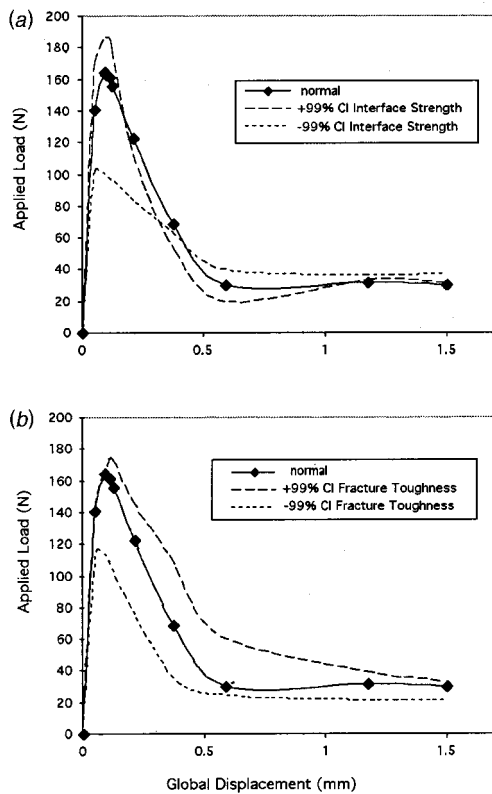
Fig. 7 Parametric finite element studies of the cement-bone structures where interface strength (a) and interface fracture toughness (b) were modified from nominal values in the interface element models. The 99 percent confidence interval values shown in Fig. 3 were used in place of nominal values for each case

ment at 50 percent of the ultimate load measurements. This suggests that the shape of the post-yield response can be dependent on the magnitude of the interface strengths. When the interface fracture toughness was changed to ±99 percent confidence interval values, a corresponding increase or decrease in structural energy to failure was recorded (Fig. 7B). Changing fracture toughness values also had large effects on the predicted ultimate load, even though the interface strength values were not modified. The effect of changing fracture toughness values on the displacement at 50 percent of the ultimate load was of similar magnitude as that found for the interface strength parameter study.

In the second parametric study, both the strength and energy to failure parameters were increased to the 99 percent confidence interval values in each of the eight finite element models. In all cases, the changes resulted in increased predicted ultimate load,

energy to failure, and displacement at 50 percent of the ultimate load (Fig. 6). These are shown as error bars in the figure. Also shown is a dotted line representing a perfect correspondence between model and experiment. For the ultimate load case (Fig. 6A), inclusion of 99 percent confidence interval values in the finite element models bounded the experimental results in five of eight cases. The three cases with the largest experimentally measured loads were still under-predicted by the finite element models. Similar results were found for the energy to failure predictions (Fig. 6B). Here, the 99 percent confidence interval values resulted in predictions that bounded the experimental data in three cases, with two additional cases approaching the experimental data. The final comparison (Fig. 6C) under-predicted the displacement at 50 percent of the ultimate load in seven out of eight cases.

Discussion

The results of this study suggest that finite element models with non-linear constitutive models at the cement-bone interface could qualitatively reproduce the structural response of physical experiments. The models were most successful in predicting the ultimate load of the experimental specimens. For the eight test specimens, the finite element models with an average error of 23.9 percent could predict 80 percent of the variability in the experimentally measured ultimate load. However, the models were least successful in predicting the energy to failure and the shape of the post-yield response.

The finite element models used in this study relied on non-linear constitutive models at the cement-bone interface to reproduce the structural response of the experimental specimens. In turn, the non-linear constitutive models used a set of experimental data relating the strength and toughness of the interface with the local morphology of the interface (quantity of interdigitated bone). Thus there were two main sources of error in the predictive capabilities of the finite element models. First, the shape of the constitutive model response may not adequately be reflected in the current model. Second, the magnitudes associated with parameters describing this constitutive model response could be in error.

In the present study we assumed a piecewise linear response of the cement-bone interface to describe the failure mechanism. In simple tensile or shear experiments of small cement-bone specimens, a wide range of post-yield responses have been noted, from linear to exponential decays from a peak load. Unfortunately, there was poor correlation ($r^2 = .012$ to 0.044) between the post-yield response and any of the parameters measured to describe the cement-bone interface [19]. Due to the lack of good predictors of the post-yield response, we chose a linear response. Further improvements in the predictive capabilities of the post-yield response could be made through improved characterization of the cement-bone interface [28].

The values assigned to the strength and toughness parameters in the interface models were based on regression relationships that were statistically significant, but still with a substantial amount of experimental scatter. The models were first analyzed using the

Table 2 The change in global structural response after interface strength and fracture toughness were adjusted based on ±99 percent confidence intervals of the quantity of interdigitated bone relationships (Fig. 3). Interface strength and interface fracture toughness were adjusted independently in this parametric study

Interface Parameter Modified	Change in ultimate load (%)	Change in energy to failure (%)	Change in displacement at 50% of ultimate load (%)
Interface Strength+99% Confidence Interval	+13.5	3.9	−20.4
Interface Strength−99% Confidence Interval	−37.9	−7.7	42.7
Interface Fracture Toughness +99%Confidence Interval	+5.4	+33.2	+39.1
Interface Fracture Toughness −99% Confidence Interval	−30.2	−33.1	−13.5

mean predicted strength and toughness values, with values assigned for twelve cement-bone interface regions in each model. As a measure of the effect of the scatter in these relationships, we assigned interface strength and toughness parameters using 99 percent confidence interval values of the mean and slope of the regression relationships. Changes in the structural response using these 99 percent confidence interval values were as large as 43 percent of nominal values. However, using 99 percent confidence interval values only provides a first estimate of the possible variability. Experimentally, there were many members of the population sample that extended beyond the confidence interval bounds (Fig. 3). Thus, even larger changes in the structural response of the finite element models could be expected. The predictive errors from the finite element models were quite low in comparison to the possible errors based on the interface model regression relationships. This suggests that the averaging affect over the entire cement-bone interface may have reduced the errors in the finite element results presented here. Nonetheless, the fact that the finite element predictions with 99 percent confidence interval bounds did not span the experimentally measured parameters for many of the cases studied here suggests that further improvement in the assignment of interface model parameters is needed to improve the capabilities of this approach.

To the authors' knowledge, there have not been other studies where the validity of computational models have been assessed for complex cement-bone structures. However, finite element modeling has been used to predict the failure response of whole bone structures such as the proximal femur and spine vertebrae. Lotz and coworkers [29] used QCT based non-linear finite element models of the proximal femur to predict the onset of structural yielding and load to fracture. For two specimens loaded to simulate a fall, errors between finite element models and experiments were between 4 percent and 22 percent. Using much more refined finite element models, Keyak et al. [30] found a strong positive correlation ($r^2 = 0.75$, $p < 0.0001$) between finite element predicted fracture load and experimental fractured load for 17 proximal femurs tested in a stance configuration. The predicted fracture strength was often underestimated for these models (a typical error was on the order of 50 percent), and was attributed to differences in the point of measurement between the model and experiments. In a different study [31], CT based finite element models of vertebral sections were also used successfully to correlate yield strength ($r^2 > 0.86$) of corresponding experimental specimens. Errors between the finite element analysis and experiment in predicting yield strength was reported to be typically within 25 percent for the 18 specimens tested. The results of the present investigation, in terms of level of correlations and prediction errors for ultimate load, appear to be of similar magnitude as the whole bone studies described above.

One difficulty with the models mentioned above and the work performed here is that they are dependent on the inherent variability in the CT density-material property relationships. For trabecular bone, a moderate to strong correlation ($r^2 = 0.58$ to 0.78) between QCT density and bone specimen strength has been found with relative errors between 34 and 56.5 percent [23]. Some of the variability is thought to be due to errors in mechanical testing technique [32]. Improvements in predicting bone strength are also possible through use of direct apparent density measures, or direct measure of specimen elastic modulus. For example, for trabecular bone specimens subjected to combined tensile and shear loading, Fenech and Keaveny [33] found relative errors of 5 percent in prediction of bone strength after normalizing the applied stress by the bone specimen elastic modulus. This would suggest that if some direct measure of non-destructive mechanical properties were possible for the cement-bone interface, then the predictive capabilities of the q_{int} versus strength or energy relationship could be improved. However, if the goal is to eventually use this approach to predict the failure process of cemented joint replacements, then the direct measure of interface or bone material properties would not be possible.

In addition to the issues mentioned above, there were several other limitations of this study. No biological changes that may occur at the cement-bone interface were included in this study. Retrievals of well-fixed femoral components have revealed intact cement-bone interfaces [2], but once yield of the cement-bone interface is reached, there may be biological changes to the interface in additional to mechanical degradation. All testing was conducted under quasi-static single-cycle loading and did not include any fatigue loading. Certainly the loading of the cement-bone interface *in vivo* will experience cyclic loading as the primary loading mechanism. Future testing for constitutive model development and for computational modeling should incorporate fatigue loading in the failure response. Cementing was performed under ideal conditions, both in the present study and in the previous work used to develop the constitutive models. Cement-bone specimens prepared in the presence of blood, marrow, or venous back pressure could affect the mechanical strength of the cement-bone interface [34]. Only one bone was used in this study, so comparisons between the response for different donors could not be tested. However, in previous experiments with simple tensile or shear tests [21], we found that bone donor was not a significant covariate after the quantity of cement-bone interdigitation was included in regression models. Therefore, the finite element models and experimental results found for the one bone used in this study should be equally effective for other bones from different donors.

In summary, it appears that the non-linear fracture mechanics approach presented here is generally successful in predicting the strength of complex cement-bone structures, but is less useful in predicting the post-yield response of these structures. Improvements in the specificity of the post-yield behavior of the cement-bone interface are needed to further improve the predictive capabilities of these models. Therefore, future work with these interface models should aim to enhance the post-yield predictions through additional morphological information about the regions of cement interdigitated with trabecular bone and bone adjacent to the cement. Direct measurement of interface morphology would be a first step towards this goal. A second goal could be to extend the current models to fully three-dimensional structures, such as cemented total hip replacements where the interface elements could be assigned properties based on regional variations in cement-bone interdigitation. With this approach, the initiation and progression of cement-bone interface failure could be determined for these structures.

References

[1] Robinson, R. P., Lovell, T. P., Green, T. M., and Bailey, G. A., 1989, "Early Femoral Component Loosening in DF-80 Total Hip Arthroplasty," J. Arthroplasty, **4**(1), pp. 55–64.

[2] Jasty, M., Maloney, W. J., Bragdon, C. R., Haire, T., and Harris, W. H., 1990, "Histomorphological Studies of the Long-Term Skeletal Responses to Well Fixed Cemented Femoral Components," J. Bone Jt. Surg., **72B**(8), pp. 1220–1229.

[3] Hori, R. Y., and Lewis, J. L., 1982, "Mechanical Properties of the Fibrous Tissue Found at the Bone-Cement Interface following Total Joint Replacement," J. Biomed. Mater. Res., **16**(6), pp. 911–927.

[4] Huiskes, R., Verdonschot, N., and Nivbrant, B., 1998, "Migration, Stem Shape, and Surface Finish in Cemented Total Hip Arthroplasty," Clin. Orthop., **355**, pp. 103–112.

[5] Herman, J. H., Sowder, W. G., Anderson, D., Appel, A. M., and Hopson, C. N., 1989, "Polymethylmethacrylate-Induced Release of Bone-Resorbing Factors," J. Bone Jt. Surg., **71-A**(10), pp. 1530–1541.

[6] Horowitz, S. M., Doty, S. B., Lane, J. M., and Burstein, A. H., 1993, "Studies of the Mechanism by which the Mechanical Failure of Polymethylmethacrylate leads to Bone Resorption," J. Bone Jt. Surg., **75-A**(6), pp. 802–813.

[7] Dohmae, Y., Bechtold, J. E., and Sherman, R. E., 1988, "Reduction in

Cement-Bone Interface Shear Strength between Primary and Revision Arthroplasty," Clin. Orthop., **236**, pp. 214–240.

[8] Bean, D. J., Hollis, J. M., Woo, S. L.-Y., and Convery, F. R., 1988, "Sustained Pressurization of Polymethylmethacrylate: A Comparison of Low- and Moderate-Viscosity Bone Cements," J. Orthop. Res., **6**(4), pp. 580–584.

[9] Köbel, R., Bergmann, G., and Boenick, U., 1976, *Mechanical Engineering of the Cement-Bone Bond, Engineering in Medicine*, M. Schldach and D. Hohman, eds., Springer-Verlag, New York, pp. 347–357.

[10] Wang, X., and Agrawal, C. M., 2000, "A Mixed Mode Fracture Toughness Test of Bone-Biomaterial Interfaces," J. Biomed. Mater. Res., **53**(6), pp. 664–672.

[11] Clech, J. P., Keer, L. M., and Lewis, J. L., 1985, "A Model of Tension and Compression Cracks with Cohesive Zone at a Bone-Cement Interface," ASME J. Biomech. Eng., **107**(2), pp. 175–182.

[12] Kanninen, M. F., and Popelar, C. H., 1985, *Advanced Fracture Mechanics*, Oxford University Press, New York.

[13] Mann, K. A., Werner, F. W., and Ayers, D. C., 1997, "Modeling the Tensile Behavior of the Cement-Bone Interface," ASME J. Biomech. Eng., **119**(2), pp. 175–178.

[14] Mann, K. A., Allen, M. J., and Ayers, D. C., 1998, "Pre-Yield and Post-Yield Shear Behavior of the Cement-Bone Interface," J. Orthop. Res., **16**(3), pp. 370–378.

[15] Broek, D., 1991, *Elementary Engineering Fracture Mechanics*, Kluwer Academic Publishers, Boston.

[16] Harrigan, T. P., and Harris, W. H., 1991, "A Three-Dimensional Non-Linear Finite Element Study of the Effect of Element-Prosthesis Debonding in Cemented Femoral Total Hip Components," J. Biomech., **24**(1), pp. 1047–1058.

[17] Brown, T. D., Pedersen, D. R., Radin, E. L., and Rose, R. M., 1988, "Global Mechanical Consequences of Reduced Cement/Bone Coupling Rigidity in Proximal Femoral Arthroplasty: A Three-Dimensional Finite Element Analysis," J. Biomech., **21**(2), pp. 115–129.

[18] Verdonschot, N., and Huiskes, R., 1996, "Mechanical Effects of Stem-Cement Interface Characteristics on Total Hip Replacement," Clin. Orthop., **329**, pp. 326–336.

[19] Mann, K. A., Ayers, D. C., Werner, F. W., Nicoletta, R. J., and Fortino, M. D., 1997, "Tensile Strength of the Cement-Bone Interface Depends on the Amount of Bone Interdigitated with PMMA Cement," J. Biomech., **30**(4), pp. 339–346.

[20] Lotz, J. C., Gerhart, T. N., and Hayes, W. C., 1990, "Mechanical Properties of the Trabecular Bone from the Proximal Femur: A Quantitative CT Study," J. Comput. Assist. Tomogr., **14**, pp. 107–114.

[21] Mann, K. A., Werner, F. W., and Ayers, D. C., 1999, "Mechanical Strength of the Cement-Bone Interface is Greater in Shear than in Tension," J. Biomech., **32**(11), pp. 1251–1254.

[22] Lewis, G., 1997, "Properties of Acrylic Bone Cement: State of the Art Review," J. Biomed. Mater. Res., **38**(2), pp. 155–82.

[23] Mow, V. C., and Hayes, W. C., 1991, Basic Orthopaedic Biomechanics, Raven Press, New York.

[24] Wong, P. C. W., Kulhawy, F. H., and Ingraffea, A. R., 1989, "Numerical Modeling of Interface Behavior for Drilled Shaft Foundations under Generalized Loading," Foundation Engineering: Current Principles and Practices, F. H. Kulhawy, ed., ASCE, New York, pp. 565–579.

[25] Keaveny, T. M., and Bartel, D. L., 1994, "Fundamental Load Transfer Patterns for Press-Fit, Surface-Treated Intra-Medullary Fixation Stems," J. Biomech., **27**(9), pp. 1147–1158.

[26] Mann, K. A., Bartel, D. L., Wright, T. M., and Burstein, A. H., 1995, "Coulomb Frictional Interfaces in Modelling Cemented Total Hip Replacements: A More Realistic Model," J. Biomech., **28**(9), pp. 1067–1078.

[27] Boone, T. J., Wawrzynek, P. A., and Ingraffea, A. R., 1986, "Simulation of the Fracture Process in Rock with Application to Hydrofracturing," Int. J. Rock Mech. Min. Sci. Geomech. Abstr., **23**(3), pp. 255–265.

[28] Maher, S. A., and McCormack, B. A. O., 1999, "Quantification of Interdigitation at Bone Cement/Cancellous Bone Interfaces in Cemented Femoral Reconstructions," Proceedings of the Institute of Mechanical Engineers, 213, pp. 347–354.

[29] Lotz, J., Cheal, E., and Hayes, W., 1991, "Fracture Prediction for the Proximal Femur using Finite Element Models: Part II-Nonlinear analysis," ASME J. Biomech. Eng., **113**(4), pp. 361–365.

[30] Keyak, J., Rossi, S., Jones, K., and Skinner, H., 1998, "Prediction of Femoral Fracture Load using Automated Finite Element Modelling," J. Biomech., **31**(2), pp. 125–133.

[31] Silva, M., Keaveny, T., and Hayes, W., 1998, "Computed Tomography-Based Finite Element Analysis Predicts Failure Loads and Fracture Patterns for Vertebral Sections," J. Orthop. Res., **16**(3), pp. 300–308.

[32] Keaveny, T. M., and Hayes, W. C., 1993, "A 20-year Perspective on the Mechanical Properties of Trabecular Bone," ASME J. Biomech. Eng., **115**(4B), pp. 534–542.

[33] Fenech, C. M., and Keaveny, T. M., 1999, "A Cellular Solid Criterion for Predicting the Axial-Shear Failure Properties of Bovine Trabecular Bone," ASME J. Biomech. Eng., **121**(4), pp. 414–422.

[34] Majkowski, R. S., Miles, A. W., Bannister, G. C., Perkins, J., and Taylor, G. J. S., 1993, "Bone Surface Preparation in Cemented Joint Replacement," J. Bone Jt. Surg., **75B**(3), pp. 459–463.